Molecular Psychiatry
https://doi.org/10.1038/s41380-018-0123-4

ARTICLE

Exploring the neuropsychiatric spectrum using high-content functional analysis of single-cell signaling networks

Santiago G. Lago[1] · Jakub Tomasik[1] · Geertje F. van Rees[1] · Jordan M. Ramsey[1] · Frieder Haenisch[1] · Jason D. Cooper[1] · Jantine A. Broek[1] · Paula Suarez-Pinilla[2,3] · Tillmann Ruland[4] · Bonnie Auyeug[5,6] · Olya Mikova[7] · Nikolett Kabacs[8] · Volker Arolt[4] · Simon Baron-Cohen[5,9] · Benedicto Crespo-Facorro[2,3] · Sabine Bahn[1]

Received: 13 October 2017 / Revised: 4 May 2018 / Accepted: 25 May 2018

Abstract

Neuropsychiatric disorders overlap in symptoms and share genetic risk factors, challenging their current classification into distinct diagnostic categories. Novel cross-disorder approaches are needed to improve our understanding of the heterogeneous nature of neuropsychiatric diseases and overcome existing bottlenecks in their diagnosis and treatment. Here we employ high-content multi-parameter phospho-specific flow cytometry, fluorescent cell barcoding and automated sample preparation to characterize ex vivo signaling network responses ($n = 1764$) measured at the single-cell level in B and T lymphocytes across patients diagnosed with four major neuropsychiatric disorders: autism spectrum condition (ASC), bipolar disorder (BD), major depressive disorder (MDD), and schizophrenia (SCZ; $n = 25$ each), alongside matched healthy controls ($n = 100$). We identified 25 nodes (individual cell subtype–epitope–ligand combinations) significantly altered relative to the control group, with variable overlap between different neuropsychiatric diseases and heterogeneously expressed at the level of each individual patient. Reconstruction of the diagnostic categories from the altered nodes revealed an overlapping neuropsychiatric spectrum extending from MDD on one end, through BD and SCZ, to ASC on the other end. Network analysis showed that although the pathway structure of the epitopes was broadly preserved across the clinical groups, there were multiple discrete alterations in network connectivity, such as disconnections within the antigen/integrin receptor pathway and increased negative regulation within the Akt1 pathway in $CD4^+$ T cells from ASC and SCZ patients, in addition to increased correlation of Stat1 (pY701) and Stat5 (pY694) responses in B cells from BD and MDD patients. Our results support the "dimensional" approach to neuropsychiatric disease classification and suggest potential novel drug targets along the neuropsychiatric spectrum.

Introduction

Neuropsychiatric diagnoses do not fall into discrete clinical groups. They represent a spectrum of conditions with overlapping symptoms shared across different clinical dimensions [1, 2]. The persistent and formidable difficulties

These authors contributed equally: S.G. Lago, J. Tomasik

Electronic supplementary material The online version of this article (https://doi.org/10.1038/s41380-018-0123-4) contains supplementary material, which is available to authorized users.

✉ Sabine Bahn
sb209@cam.ac.uk

1 Department of Chemical Engineering and Biotechnology, University of Cambridge, Cambridge, UK

2 Department of Psychiatry, Marqués de Valdecilla University Hospital, IDIVAL, School of Medicine, University of Cantabria, Santander, Spain

3 Centro de Investigación Biomédica en Red de Salud Mental (CIBERSAM), Santander, Spain

4 Department of Psychiatry and Psychotherapy, University of Münster, Münster, Germany

5 Autism Research Centre, Department of Psychiatry, University of Cambridge, Cambridge, UK

6 Psychology Department, Edinburgh University, Scotland, UK

7 Foundation Biological Psychiatry, Sofia, Bulgaria

8 Cambridgeshire and Peterborough NHS Foundation Trust, Cambridge, UK

9 CLASS Clinic, Cambridgeshire and Peterborough NHS Foundation Trust, Cambridge, UK

Published online: 23 July 2018

associated with neuropsychiatric nosology are profound, with distinctions between bipolar and unipolar depression or autism and childhood schizophrenia being formally recognized only since the 1950s and 1970s respectively [3, 4]. Today, 20% of individuals who meet the criteria for one condition in the Diagnostic and Statistical Manual of Mental Disorders IV (DSM-IV) [5] also fulfill the criteria for at least two more [2]. Moreover, the decision to class a patient in a given diagnostic group is based on subjective observations of behavioral symptoms at the discretion of medical practitioners and is not an objective measure of biological etiology [6]. This results in a lack of diagnostic stability, exemplified by up to 50% of psychotic patients switching diagnosis over a 10 year period [7], and highlights the fact that differential diagnosis is a more persistent bottleneck in clinical psychiatry relative to case–control definition. In many cases, the diagnosis is ultimately defined by relative response to treatment following successive rounds of pharmacological titration across different drug classes [8]. This process can have a devastating effect on patient quality of life, with only 40–60% of patients achieving substantial remission of symptoms [9]. Furthermore, due to the limited understanding of the heterogeneous pathophysiology of neuropsychiatric diseases, incomplete characterization of the molecular targets of existing drugs and a lack of relevant preclinical models, mechanistically novel drug entities with the potential to address treatment resistance have not been forthcoming.

While recent advances of genetic association data have provided unprecedented insights into the potential molecular mechanisms underlying neuropsychiatric pathogenesis and drug action, aggregate genomic risk profiling of single-nucleotide polymorphisms (SNPs) still only accounts for a small proportion (0.17–0.28) of disease liability relative to the heritable risk (0.37–0.81) observed in monozygotic twin and family studies across different conditions, including autism spectrum condition (ASC), bipolar disorder (BD), major depressive disorder (MDD), schizophrenia (SCZ), and attention-deficit hyperactivity disorder (ADHD) [10]. Furthermore, the discovery that each neuropsychiatric patient has a different combination of common but weak, or rare but highly penetrant, risk alleles [11–13] highlights the challenge of identifying points of functional convergence which represent potentially meaningful molecular drug targets. This difficulty is further compounded by the fact that genetic risk alleles are often shared between related neuropsychiatric conditions [10], as exemplified by the finding that voltage-gated calcium channel subunits CACNA1C and CACNB2 were amongst the top loci implicated in a combined cohort of five different neuropsychiatric diseases (BD, MDD, SCZ, ASC, and ADHD) relative to controls [14]. Thus, one of the primary challenges to adequately contextualizing neuropsychiatric drug target selection is determining which functional targets are unique to a given condition and which are shared between multiple conditions. The second imperative challenge, as the dimensionality of the molecular landscape of neuropsychiatric diseases becomes apparent, is to find a means of placing individual patients with partially overlapping symptomatology into therapeutic categories that align more closely with treatment response. In order to address these challenges, it is necessary to progress from the single disease case–control design, prevalent in many molecular profiling studies, and explore multiple neuropsychiatric diseases in parallel at the level of drug target identification.

Given their genomic complexity and the difficulties of accessing live human brain tissue, there has been a paucity of relevant cellular models in which to explore functional alterations in cellular physiology and drug response in neuropsychiatric conditions. However, evidence suggesting that neuropsychiatric conditions are systemic with functional alterations of cellular physiology manifested in the central nervous system (CNS) as well as peripheral tissues [15–17], has provided new opportunities to address these obstacles. One such strategy, using induced pluripotent stem cell (iPSC) technology, involves the reprogramming of peripheral somatic cells from neuropsychiatric patients to CNS lineage cells. While this has offered novel insights into cellular pathology and drug treatment response [18–20], this approach is limited by relatively high cost, low throughput and phenotypic inconsistencies arising from extended cell culture protocols [21, 22]. In addition, functional characterization of iPSC-derived neuronal lineages has focused on a limited number of readouts (e.g., electrophysiology or neurotransmitter release) relating to pre-existing hypotheses [23]. In contrast, native peripheral blood mononuclear cells (PBMCs) are a readily accessible primary tissue which has been shown to express many CNS receptors and downstream signaling proteins which are implicated in neuropsychiatric disease [24, 25]. Furthermore, a recent genome-wide association study (GWAS) suggested the enrichment of SNPs associated with neuropsychiatric (SCZ) risk loci within PBMC subtype (B cell)-specific gene expression enhancers [11]. Moreover, evidence that peripheral alterations can induce functional changes in the CNS with corresponding behavioral symptomatology (e.g., psychotic symptoms linked to gut microbiome alterations [26] or depressive-like symptoms following pro-inflammatory cytokine release during microbial infection [27, 28]) suggests that peripheral cellular models might not be confined solely to surrogate identification of CNS targets, but might also represent underlying pathophysiological mechanisms. Importantly, PBMCs are amenable to high-content functional screening allowing unbiased examination of a wide range of cellular response mechanisms, as evidenced by parallel applications in hematological malignancies [29] and autoimmune conditions [30].

Exploration of functional alterations which reflect the disease state, in neuropsychiatric patient PBMCs, could have important implications for overcoming present obstacles in neuropsychiatric drug target identification. First, functional testing in live cells has the potential to reveal relevant disease-specific alterations in cell signaling networks which are not detectable by quantification of basal protein levels in the resting state, including regulatory and homeostatic mechanisms [29]. Second, the focus on cellular responses provides the opportunity to summarize complex genetic risk factors, with heterogeneous manifestations, as integrated phenotypes which are more amenable to drug screening [31]. Third, targeting of key functional mediators within the cell, such as protein kinases, phosphatases, ion channels, and G protein-coupled receptors, represents a heuristic screening method focused on the most "druggable" part of the genome [32]. Finally, the use of primary cells from patients at the initial stage of drug target identification could potentially yield a higher success rate of candidate compounds in subsequent stages of the drug discovery pipeline [33].

Here we apply high-content, single-cell screening of functional ligand–receptor interactions and downstream signaling mechanisms [25, 34, 35] to explore differences in cell signaling dynamics across the neuropsychiatric spectrum using primary PBMCs ex vivo from four major disease indications (ASC, BD, MDD, and SCZ; $n = 100$ patients, 25 per diagnosis) in addition to matched typical controls ($n = 100$). We employ multi-parameter phospho-specific flow cytometry [35], fluorescent cell barcoding [34], and automated sample preparation to simultaneously measure the activation of 42 intracellular signaling epitopes (spanning key CNS and immune cell signaling pathways such as Akt/GSK-3β, JAK/STAT, MAPK, PKA, PKC, IL-1R/TLR, and T/B cell receptor (TCR/BCR) signaling) in response to 14 functional ligand conditions (including CNS receptor agonists, antigens, cytokines, and intracellular signaling modulators) in three PBMC cell subtypes ($CD4^+$ T cells ($CD3^+CD4^+$), $CD4^-$ T cells ($CD3^+CD4^-$), and predominantly B cells ($CD3^-$)). This provided a functional matrix of 1764 unique cell subtype–epitope–ligand combinations ("nodes"), in addition to the basal expression levels of each epitope per cell subtype, measured in each PBMC sample across the five clinical groups. We explore the utility of this functional array in three ways. First, we assess the degree of overlap between the cell signaling profile of different neuropsychiatric conditions relative to each other and controls, based on individual donor readouts. Second, we examine the cell signaling nodes that were most significantly altered in one or more disease indication(s) for each PBMC cell subtype. Finally, we explore putative alterations in cell signaling network connectivity across each of the major neuropsychiatric conditions.

Materials and methods

Clinical sample recruitment

Patients and matched typical control PBMC donors were recruited as follows: ASC (Cambridge Autism Research Centre, Cambridge University, Cambridge, UK; $n = 25$/group), BD (Foundation Biological Psychiatry, Sofia, Bulgaria; $n = 13$ patients and $n = 15$ controls; and Union House, Cambridgeshire and Peterborough Mental Health Foundation Trust, Cambridge, UK; $n = 12$ patients and 10 controls), MDD (Westfälische Wilhelms University Hospital, Münster, Germany; $n = 25$/group), and first-onset antipsychotic drug-naïve SCZ (University Hospital Marqués de Valdecilla, Santander, Spain; $n = 25$/group; Tables S3 and S4). In the BD cohort, patients and respective controls from different clinical centers were matched within and between centers for age, sex, and body mass index (BMI). The medical faculty ethical committees responsible for the respective sample collection sites approved the study protocols. Informed consent was given in writing by all participants and clinical investigations were conducted according to the Declaration of Helsinki [36] and Standards for Reporting of Diagnostic Accuracy [37].

Diagnoses of neuropsychiatric pathology were conducted by experienced psychiatrists and were based on the Diagnostic and Statistical Manual of Mental Disorders-IV-Text Revision (DSM-IV-TR) [5]. The exclusion criteria for patients and controls included: age below 18 years old, additional neuropsychiatric diagnoses, other neurological conditions including epilepsy, mental retardation, multiple sclerosis, immune/autoimmune conditions, infectious disease, metabolic conditions including diabetes, obesity, cardiovascular disease, hepatic and renal insufficiency, gastrointestinal conditions, endocrine conditions including hypo-/hyperthyroidism and hypo-/hypercortisolism, respiratory diseases, cancer, severe trauma, substance abuse including psychotropic drugs and alcohol, somatic medication for non-CNS indications with CNS side-effects and somatic medication affecting the immune system including glucocorticoids, anti-inflammatory/immuno-modulating drugs, and antibiotics.

PBMC isolation and culture

PBMCs were prepared within 4 h from blood collected into 7.5 ml sodium heparin tubes (BD Biosciences; ASC, BD, and MDD) or acid citrate dextrose solution A tubes (BD Biosciences; SCZ). Whole blood was pelleted at 500 g for 10 min to remove platelet-rich plasma, diluted 1:1 with Dulbecco's phosphate-buffered saline solution (PBS; Sigma-Aldrich) and centrifuged over Ficoll-Paque PLUS (GE Healthcare) at 750 g for 20 min at 23°C (15 min at 1000 g for BD samples from Sofia). PBMCs were extracted

from the interphase, washed three times with PBS at 300 g for 10 min (once at 760 g for 10 min for BD samples from Sofia) and cryopreserved at $5*10^6$ cells/ml in heat-inactivated fetal bovine serum (FBS; Sigma-Aldrich) (Roswell Park Memorial Institute (RPMI)-1640 medium with 25 mM Hepes, Ultraglutamin-1, 10% FBS and 1% penicillin–streptomycin for BD samples from Sofia) containing 10% dimethyl sulfoxide (DMSO; Sigma-Aldrich). PBMCs were thawed at 37°C and resuspended in sterile conditions in complete RPMI media with deoxyribonuclease (DNAse) (RPMI-1640 with sodium bicarbonate (Sigma-Aldrich), 10% FBS (Life Technologies), 50 U/ml penicillin and 50 µg/ml streptomycin (Life Technologies), 2 mM L-alanyl-L-glutamine dipeptide (Life Technologies), and 20 µg/ml DNAse (Sigma-Aldrich)). The cells were counted using a Coulter Counter (Beckman Coulter), pelleted and resuspended at $2*10^6$ cells/ml. The cells were strained via a 40 µm cell strainer (Corning) and rested for 24 h at 37°C/5% CO_2 in 96-well polypropylene plates (Starlab). Samples from participants from different clinical groups ($n = 200$), alongside QC samples ($n = 16$) from a single typical control donor, were randomized across different plates, plate positions and experimental days to minimize measurement-related batch effects.

Preparation of functional ligands

Ligands ($n = 14$) used to stimulate PBMCs were selected following an initial screen of 56 stimulants [25] and included broad-range as well as specific cell signaling activators/inhibitors, cell type-specific antigens, and CNS receptor agonists/antagonists. Ligands were purchased from BD Biosciences, Sigma-Aldrich, Tocris/Bio-Techne, eBioscience/Affymetrix, Life Technologies, Antibodies-online, and Enzo Life Sciences. JB1121 was synthesized following published protocols [38] and supplied courtesy of Joshua A. Bishop, Tracey Petryshen, and Steven J. Haggarty from Harvard Medical School (Boston, MA, USA). Table S1 lists the ligands used with their primary mechanisms of action and final assay concentrations (selected based on published in vitro efficacy data). Stock solutions of ligands were prepared in sterile conditions. Initial solubilization was achieved using DMSO (for small molecules) or PBS (for biologicals). Intermediate dilutions were made in PBS and DMSO was added to equivalent amounts for each ligand and vehicle. All stocks and dilutions of ligands were stored at −80°C and repeated freeze–thaw cycles were avoided.

Stimulation of PBMCs

Stimulation is defined broadly as the exposure of PBMCs to a ligand which has the potential to perturb the resting state cell signaling dynamics by either increasing or decreasing the expression of cell signaling epitopes. PBMCs were pelleted and resuspended in 96-well polypropylene plates using complete RPMI media without penicillin–streptomycin at $3*10^6$ cells/ml. The cells were rested for 45 min at 37°C before ligand exposure.

Ligands and vehicle were reconstituted in complete RPMI media without penicillin–streptomycin and added to the cells using a Biomek NX liquid handler (Beckman Coulter) with integrated compact shaker–heater–cooler system (Inheco). The final concentration of DMSO was 0.1%. Vehicle wells represented one eighth of the total wells assayed and were spaced evenly across each 96-well plate. The cells were exposed to the ligands at 37°C for 30 min. For wells treated with the anti-CD3/CD28-XL ligands, the final 2 min of the resting period were used to pre-incubate the cells with biotinylated anti-CD3 (OKT3)/anti-CD28 (CD28.2) antibodies (eBioscience), before cross-linking them using neutravidin (Life Technologies) in the stimulation step. Ligand exposure was halted by fixation for 10 min at 37°C using paraformaldehyde (Sigma-Aldrich) in PBS at a final concentration of 1.6%.

Fluorescent cell barcoding

Stock solutions of barcoding dyes CBD 450 (BD Biosciences) and CBD 500 (BD Biosciences) were prepared as per the manufacturer's instructions in DMSO in polypropylene 96-well plates and stored at −80°C. Different combinations of the dyes were used to produce 16 barcoded cell populations resolved using final concentrations of CBD 450 (0.000, 0.015, 0.050, 0.150 mg/ml) combined with CBD 500 (0.000, 0.038, 0.125, 0.375 mg/ml; Figure S1). Fixed cells were washed with PBS and permeabilized in 100 µl ice cold methanol (Fisher Chemical) for 20 min at 2°C using a Biomek NX liquid handler. The barcoding dyes were diluted in ice cold PBS and 100 µl/well was added to the suspension of cells in methanol. The final concentration of DMSO from the barcoding dyes at this stage was 3.5%. The barcoding reaction was incubated in the dark for 30 min at 2°C and the cells were washed five times in ice cold FACS buffer (PBS with 0.5% bovine serum albumin (Sigma-Aldrich)). The barcoded cells from individual donors were pooled and pelleted.

Intracellular staining of cell signaling epitopes in PBMC subsets

The pooled fixed-permeabilized-barcoded cells were resuspended in 100 µl of FACS buffer containing 20% human Fc receptor binding inhibitor (eBioscience) and incubated for 20 min at room temperature in the dark. The cells were stained using 1 µl/ml anti-human CD3 (UCHT1) PE-Cy7

(eBioscience) and 1 µl/ml anti-human CD4 (SK3) PerCP-eFluor710 (eBioscience) and distributed across a 96-well polypropylene plate. The cells were stained using a Biomek NX liquid handler with fluorescently conjugated anti-human antibodies against intracellular signaling epitopes (Table S2) for 45 min in the dark at room temperature, as per the manufacturer's instructions. Antibodies against intracellular epitopes were purchased from BD Biosciences, Cell Signaling Technology and Merck Millipore and were used in groups of three antibodies per plex. The cells were washed twice and resuspended in FACS buffer at $2*10^6$ cells/ml for acquisition.

Data acquisition using flow cytometry

PBMC cell suspensions were acquired using an eight color FACSVerse flow cytometer (BD Biosciences) with 405, 488, and 640 nm laser excitation at an average flow rate of 2 µl/s and an average threshold event rate of 1000–2000 events/s. Each experiment was done once and single acquisition was conducted per condition. Multicolor Cytometer Setup and Tracking beads (BD Biosciences) were used for QC and standardization of photomultiplier tube detector voltages across multiple experimental runs. Fluorescence compensation was conducted using anti-mouse IgGκ antibody capture beads (Bangs Laboratories) labeled separately with anti-human CD3 (UCHT1) PE-Cy7, anti-human CD4 (SK3) PerCP-eFluor-710, anti-human Stat3 (pY705) (4/P-STAT3) AlexaFluor488 (AF 488; BD Biosciences), anti-human Stat3 (pY705) (4/P-STAT3) PE (BD Biosciences), and anti-human Stat3 (pY705) (4/P-STAT3) AlexaFluor647 (AF 647; BD Biosciences), alongside single-stain controls with maximum and minimum concentrations of each barcoding dye per PBMC sample.

Statistical data analysis

Flow cytometry data was analyzed in FCS 3.0 file format using Flow Jo v.10.0.8 software (Tree Star). Statistical analysis was conducted using R v.3.3.0 software (R Core Team) [39] and GraphPad Prism 5 (GraphPad Software Inc.). Sample sizes were chosen based on previous work [25]. PBMC samples in which the lymphocyte gate contained less than 30% of events, measured by forward scatter (FSC-A)/side scatter (SSC-A), were excluded from further analysis. Experimental variables including positional effects within and across 96-well plates, barcoding dye fluorescence spillover, sample viability, cell counts, clinical group, and sample source were investigated using principal component analysis (Figure S2). Batch effects in median fluorescence intensities (MFIs) caused by running samples from different countries of origin and on different days were normalized for each epitope and barcode using the empirical Bayes algorithm—ComBat (R "sva" package; Figure S3) [40, 41], which is well established for removing sample origin and batch effects in a range of high-impact studies [42–49]. Matching of clinical groups was conducted using the Wilcoxon rank-sum test (Kruskal–Wallis test for more than two groups) for continuous variables or the Fisher's exact test (χ^2 test for more than two groups) for categorical variables. The minimum number of individual PBMC donors included in any of the comparisons was 15. All statistical tests were two sided where applicable.

For the determination of ligand activity, the MFIs across PBMC samples, within each clinical group, cell subtype and stained epitope, were compared between each ligand and the vehicle treatment using the mixed effects analysis of covariance (mixed ANCOVA; accounting for replicate measurements). Relevant covariates were selected amongst age, sex, and BMI in a stepwise procedure using Bayesian Information Criterion. The null distribution was calculated using permutation procedure ($n = 1000$ permutations) to control for small sample numbers, unknown distribution of the data and the presence of outliers. The same test was also applied for each ligand per functional fluorescence channel (AF 488, PE and AF 647) in the unstained condition to determine whether the ligand activity was an artifact of fluorescence spillover from adjacent channels or ligand auto-fluorescence (background fluorescence). In cases where the ligand MFI was significantly altered with respect to vehicle MFI in the unstained condition, the epitopes labeled in the corresponding functional channel were only counted as active if the MFI response was in a different direction or had a minimum 10% greater fold change than the unstained condition. For ligands with significant activity (permuted $P < 0.05$) which superseded the background fluorescence, the response ratio was quantified as the median MFI of the ligand condition divided by the median MFI of the vehicle condition across PBMC samples. For responses <1 (i.e., where the ligand caused a decrease in MFI with respect to the vehicle), the response is reported as a negative fold change (−1/response ratio). The stain index of each antibody, per cell subtype, was calculated across PBMC samples from all clinical groups, in the absence of stimulation, as the median MFI of the antibody stained sample divided by the median MFI of the corresponding unstained control.

For the comparison of the clinical groups, only nodes (cell subtype–epitope–ligand combinations) which showed a significant ligand activity (permuted $P < 0.05$, adjusted for background fluorescence) in any of the clinical groups, with a minimum fold change of 10% ($n = 581$), in addition to the basal epitope levels ($n = 126$), were analyzed. Although exclusive, this filter ensures that only the most robust nodes

are reported in the clinical association analysis. Association of each signaling node MFI to clinical group status was investigated using a mixed ANCOVA model, accounting for replicate measurements, after adjusting for covariates. To account for the unknown distribution of the data, the small sample size and the presence of outliers, the null distribution of the test statistic was estimated by randomly permuting sample labels 1000 times for each node. The predictive variables of clinical group and ligand presence were set as interaction term, alongside main effect terms, within the model to determine epitopes which responded differently to individual ligand exposures across the clinical groups (permuted $P < 0.05$, mixed ANCOVA F-test). Group status, without interaction, was set as the predictive variable to identify differences in basal epitope expression between clinical groups. An additional criterion of non-permuted
P value < 0.05 was applied to the F-test results to exclude nodes which gained significance as a result of permutation, despite being insignificant ($P \geq 0.05$) for non-permuted P value. Pairwise t-test comparisons within the linear mixed effects model were used to determine which clinical groups differed significantly from typical controls (permuted $P < 0.05$). Optional covariates, age, sex, and BMI were selected in a stepwise procedure for each node separately using Bayesian Information Criterion. For nodes differing significantly ($P < 0.05$, mixed ANOVA F-test) between the four cohorts of 25 control samples, in either the vehicle or the ligand condition, an additional filter was applied, including permuted $P < 0.05$ for the within-cohort disease-control comparison (mixed ANCOVA F-test; 25 patients vs. 25 controls) and a consistent within-cohort disease potentiation/attenuation fold change relative to the between-cohort comparison. Significant nodes have also been tested for their association with patient medication status and source of the sample (if samples in given group originated from more than one location) using mixed ANCOVA F-test. Q values were calculated using the Benjamini–Hochberg procedure [50]. Box plots of disease-associated nodes show interquartile range with the median (horizontal line) and the minimum and maximum values (whiskers), excluding outliers (dots).

Correlation network analysis was based on Pearson correlation coefficients between epitope readouts within each cell type, as implemented in the R "corrr" package v.0.2.1. Combined readouts from all treatment conditions, including vehicle, were used to cover a broad range of activities. The proximity of the epitopes was determined by multi-dimensional scalingand and the color and transparency of the connecting lines represent the strength of the correlation.

Data were visualized using Flow Jo, R software, Excel 2016 (Microsoft), and Adobe Illustrator (Adobe Systems).

Code availability

Upon request.

Results

Definition of the functional matrix of cell signaling responses in PBMC subsets

We first sought to examine whether the cell signaling activity profile of the ligands used in the high-content assay (Table S1), in terms of epitope and cell subtype specificity (Table S2, Figure S1) across the clinical groups (Tables S3 and S4) at the 30 min incubation time point [25], was consistent with previously published data. Positive controls (calyculin A, PMA/ionomycin, thapsigargin, and staurosporine) were the most universally active ligands ($P < 0.05$, mixed ANCOVA F–test; min. 10% fold change in epitope expression after adjusting for background fluorescence) across cell subtypes (Figure S4), consistent with their known profile as broad-spectrum cell signaling modulators [25, 51, 52]. Epitope-specific responses were observed for JAK-Stat cytokines (IL-6, IL-10, and IFN-α2c) across different Stat isotypes (Stat1, Stat3, Stat4, Stat5) [51, 52], for mTORC1 inhibitor (rapamycin) at mTORC1 substrate 4EBP1 (pT36/pT45) [53] and for cAMP pathway ligands (forskolin and NECA) at PKA RIIα (pS99) [54, 55]. Cell subtype-specific responses were observed for antigen-receptor ligands in $CD4^+$ T cells at SLP-76 (pY128), Zap-70 (pY319)/Syk (pY352), and WIP (pS488), following T-cell receptor stimulation (anti-CD3/CD28) [56, 57], and in B cells at IκBα, p38 MAPK (pT180/pY182), and S6 (pS235/pS236), following B-cell receptor stimulation (BCR/CD40L) [58, 59]. IL-6 also displayed cell subtype specificity in terms of the magnitude of phosphorylation induction at Stat1 (pY701), Stat3 (pY705), and Stat5 (pY694) epitopes, which was greatest in $CD4^+$ T cells, moderate in $CD4^-$ T cells, and absent in B cells, consistent with previous reports [51, 60]. Taken together, these data suggest that the high-content functional screening assay is capable of resolving characteristic ligand–epitope response profiles across the clinical groups.

Subsequently, we compared the total number of cell signaling responses and their distribution across the different PBMC cell subtypes between the clinical groups. The proportion of active cell signaling responses relative to the total number of functional nodes measured ($n = 1764$) was similar across clinical groups (24–26%; Table S5), with 69–75% of active nodes in each disease showing responses in the same direction across all groups. The distribution of significant cell signaling responses across the different cell subtypes, in terms of the number of active nodes and range

of fold changes (FC), was also largely conserved between the clinical groups, with $CD4^+$ T cells accounting for 34–37% of active nodes (FC −7.5 to 46.5), $CD4^-$ T cells accounting for 32–36% of active nodes (FC −7.5 to 62.6), and B cells accounting for 30–34% of active nodes (FC −7.9 to 46.7; Table S5 and Figure S5). Taken together, these data suggest that any differences between the PBMC response profiles of the different clinical groups were likely to be pathway specific and not the result of widespread changes in the activity of the measured cell subtypes.

Differences in cell signaling across the neuropsychiatric spectrum

Having defined which cell signaling nodes were active, we aimed to identify nodes which showed a significant interaction with clinical group status ($P < 0.05$, mixed ANCOVA F-test) and were significantly altered in at least one of the disease groups (ASC, BD, MDD, and SCZ) relative to typical controls ($P < 0.05$, pairwise t-test comparisons within the linear mixed effects model). Twenty-five nodes fulfilled these criteria, including 20 responses to ligand stimulation and the basal expression of five epitopes (Table S6). We then assessed the distribution of individual patient diagnoses across the identified panel of neuropsychiatric cell signaling alterations. Unsupervised hierarchical clustering of individual patient readouts across the putative disease nodes revealed four main clusters (Fig. 1a). However, patients from different disease groups did not segregate exclusively into specific clusters. Instead, they exhibited a spectral distribution across the clustering hierarchy with each clinical group showing areas of peak density in addition to varying degrees of overlap with the other clinical groups (Fig. 1b). The order of primary peaks across the disease continuum ranged from MDD on one end, through BD and SCZ, to ASC on the other end. There was a high degree of overlap between SCZ and BD and between BD and MDD, moderate overlap between SCZ and MDD and between SCZ and ASC, and little overlap between MDD and ASC and between BD and ASC.

To contextualize the differences between disease groups relative to typical controls, we performed linear discriminant analysis on the complete set of assayed nodes (Fig. 1c). This revealed considerable overlap between all clinical groups, with typical controls located centrally in the discriminant space and each disease reflected as an extension thereof. BD and MDD showed the widest range of extension in a single direction, while ASC appeared as a broad "halo" surrounding the control (Ctrl) space. Overlap of the disease space within the Ctrl area was greatest for ASC followed by BD, MDD, and lastly SCZ. Importantly, the area occupied by SCZ overlapped almost entirely with that of BD and only to a lesser extent with that of the other diseases. Taken together, these results suggest variable overlap between the cell signaling repertoires associated with different neuropsychiatric diseases, which are heterogeneously expressed at the level of each individual patient.

Disease-specific cell signaling responses in PBMC subsets

Analysis of the putative neuropsychiatric disease nodes at the level of each individual disease cohort revealed a greater number of cell signaling alterations in SCZ (14 altered nodes) relative to MDD (8 nodes), BD (6 nodes), and ASC (5 nodes; Fig. 2a, Table S6). At the level of each PBMC cell subtype, more disease-associated nodes were found in B cells (14 nodes) relative to $CD4^+$ T cells (8 nodes) and $CD4^-$ T cells (3 nodes), although the distribution of these nodes across the cell subtypes was different dependent on the disease in question (Fig. 2a, Table S6).

In terms of individual epitopes, we identified cell signaling alterations previously associated with neuropsychiatric conditions including dysregulation of total Akt1 in SCZ and altered Akt phosphorylation at pT308 in BD (Fig. 2b). Furthermore, the analysis revealed potentially novel cell signaling targets such as S6 (pS235/pS236), NF-κB p65 (pS529), and Stat3 (pS727) which were enriched among the total set of disease-associated alterations (20%, 12%, and 12% of nodes, respectively, compared to 2.4% expected by chance). The most significantly associated nodes per cell subtype revealed functional alterations of these epitopes which were either unique to single diseases, for example the attenuated $CD4^+$ T cell response to staurosporine at NF-κB p65 (pS529) in SCZ or the potentiated B cell response to thapsigargin at S6 (pS235/pS236) in MDD, or shared between multiple diseases, for example the attenuated $CD4^-$ T cell response to calyculin at S6 (pS235/pS236) in BD and SCZ (Fig. 2c). In some cases (e.g., S6 (pS235/pS236)), the same epitope responded differently in different diseases depending on the stimulant applied and cell subtype analyzed. Taken together, these findings suggest that there are ligand-specific functional responses that are altered in one or more neuropsychiatric conditions, dependent on the cell signaling epitope and PBMC subtype in question.

Altered cell signaling network connectivity across neuropsychiatric conditions

Having compared the responses at individual cell signaling nodes, we sought to explore differences in cell signaling network connectivity between typical controls and different

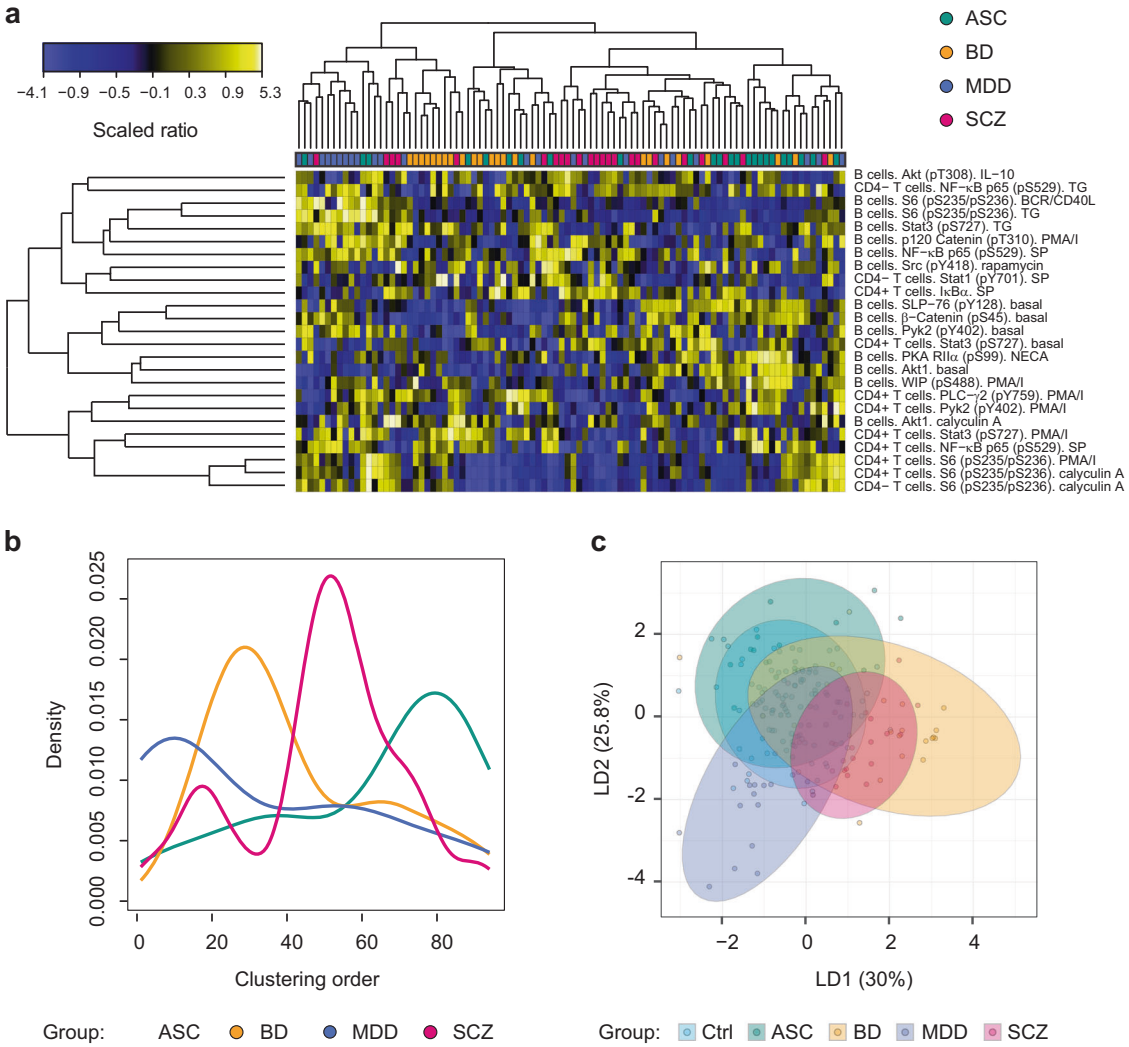

Fig. 1 Individual patient differences in cell signaling across the neuropsychiatric spectrum. **a** Hierarchical clustering of individual patient (*x* axis) peripheral blood mononuclear cell (PBMC) readouts for nodes (defined as cell subtype–epitope–ligand combinations; *y* axis) which showed a significant association with clinical group status (i.e., significant ($P < 0.05$) interaction between ligand treatment and clinical status for ligand responses or significant main effect of clinical group for basal epitope expression in mixed ANCOVA *F*-test) and were significantly altered in at least one of the clinical groups (autism spectrum condition (ASC), bipolar disorder (BD), major depressive disorder (MDD) or schizophrenia (SCZ)) relative to typical controls (Ctrl; $P < 0.05$, pairwise *t*-test comparisons within the linear mixed effects model). These included 20 ligand responses and five basal epitope expression levels. Nodes involving response to ligand were filtered for activity in at least one of the clinically associated groups, as described in Materials and methods. Legend reflects ratio of epitope median fluorescence intensity (MFI) of the ligand treatment to mean epitope MFI of the vehicle treatment (for ligand responses) or ratio of mean epitope MFI of the vehicle condition to mean epitope MFI of the vehicle condition in the control group (for basal epitope expression) per condition and sample, standardized to mean control levels and scaled across all nodes. Ligand abbreviations: BCR/CD40L, B-cell receptor stimulant/-MegaCD40 ligand; PMA/I, phorbol 12-myristate 13-acetate/ionomycin; SP, staurosporine; TG, thapsigargin. **b** Spectral summary of cell signaling overlap between different neuropsychiatric diseases. Kernel density estimates were derived from the hierarchical clustering order (**a**) to reflect the probability distributions of each condition across the clustering hierarchy. **c** Linear discriminant analysis on complete set of assayed nodes, including ligand response nodes ($n = 1764$) and basal epitope levels ($n = 126$), for all clinical groups. Dots reflect individual donors and shaded areas reflect 95% confidence intervals for each clinical group. Data in each panel (**a–c**) is color-coded in terms of clinical group identities with PBMC sample numbers as follows: autism spectrum condition (green; $n = 25$), bipolar disorder (gold; $n = 25$), major depressive disorder (purple; $n = 25$), schizophrenia (magenta; $n = 25$), and typical control (blue; $n = 100$)

major neuropsychiatric conditions. To do this, we correlated epitope responses across all ligands and individual PBMC donors for each clinical group to form putative network connections and then mapped these onto pathway clusters in principal component space. In $CD4^+$ T cells (Fig. 3), the basic pathway cluster structure was preserved across the clinical groups. However, the data revealed alterations in cell signaling network connectivity (Pearson's $r \geq 0.8$ or

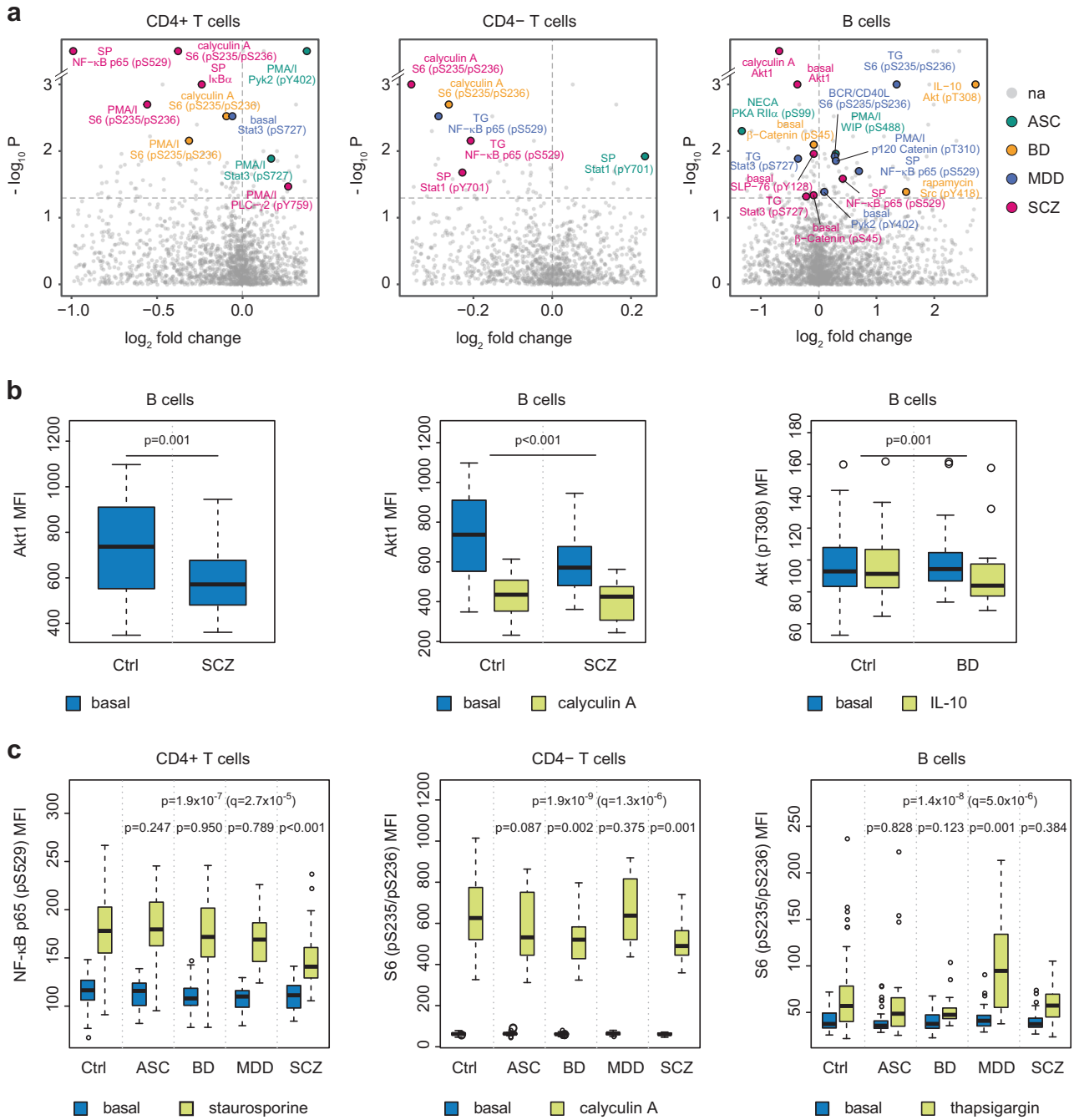

≤−0.8) for specific conditions relative to controls. Network disconnectivity was observed within the antigen/integrin (A/I) receptor pathway cluster for SCZ at IκBα–PKC-α (**1**) and Src (pY418)–PKA RIIα (pS99) (**2**), for SCZ and ASC at CrkL (pY207)–Pyk2 (pY402)–Src (pY418) (**3**), and for BD at PLC-γ1–PLC-γ2 (**4**). MDD did not show any missing epitope correlations relative to controls. Conversely, other areas of the cell signaling network showed increased connectivity in specific diseases relative to controls. This included an increasing number of negatively correlated connections between total Akt1 and adjacent epitopes in the Akt pathway cluster for MDD, SCZ, and ASC successively (**5**) and an additional positively correlated connection at PLC-γ1–Src (pY418) for SCZ and ASC in the A/I receptor cluster (**6**).

Likewise, in the other PBMC cell subtypes, while the basic pathway cluster structure was preserved between clinical groups, there were notable disease-specific alterations in cell signaling correlation networks. In $CD4^-$ cells (Figure S6), these included the disruption of an alternating positive and

◀ **Fig. 2** Comparison of disease-specific cell signaling responses in peripheral blood mononuclear cell (PBMC) subsets. **a** Disease-associated cell signaling nodes per PBMC cell subtype. Shows nodes (defined as cell subtype–epitope–ligand combinations) which displayed a significant association with disease group status (ligand treatment–clinical status interaction $P < 0.05$ for ligand responses or main effect of clinical status $P < 0.05$ for basal epitope levels in mixed ANCOVA F–test) and were significantly altered in at least one of the disease groups (autism spectrum condition (ASC), bipolar disorder (BD), major depressive disorder (MDD), or schizophrenia (SCZ), $n = 25$ each) relative to typical controls (Ctrl, $n = 100$; $P < 0.05$, pairwise t-test comparisons within the linear mixed effects model). Y axes show a -$\log_{10}$ transformation of P values for node associations between a single disease and the control group from pairwise t-test comparisons within the linear mixed effects model. X axes show $\log_2$-transformed fold changes (FC) between a single disease and the control group defined for ligand responses as an absolute value of (1−ligand response in disease group)/(1−ligand response in control group) and for basal epitope levels as median epitope MFI (median fluorescence intensity) for the vehicle condition in the disease group/median epitope MFI for the vehicle condition in the control group. For the majority of ligand responses, this represents a means of expressing the relative potentiation ($\log_2FC > 0$) or attenuation ($\log_2FC < 0$) of response independently of its direction. Nodes involving response to ligand were filtered for activity in at least one of the clinically associated groups, as described in Materials and methods. Significant nodes are annotated and color–coded in terms of clinical group identities: ASC (green), BD (gold), MDD (purple), and SCZ (magenta). Ligand abbreviations: BCR/CD40L, B cell receptor stimulant/MegaCD40 ligand; PMA/I, phorbol 12-myristate 13-acetate/ionomycin; SP, staurosporine; and TG, thapsigargin. **b** Dysregulation of putative neuropsychiatric drug targets Akt1 in SCZ (panels 1–2) and Akt (pT308) in BD (panel 3) in B cells. Plots show MFI of epitope expression (y axis) per clinical group (x axis) under basal (vehicle; blue) or ligand stimulation (yellow) conditions. Shows interaction P value for ligand responses and main effect of clinical status P value for basal epitope expression (pairwise t-test within the linear mixed effects model). **c** Five-group representation of the most significant clinically associated nodes (mixed ANCOVA F-test) in each cell subtype. Plots show MFI of epitope expression (y axis) per clinical group (x axis) under basal (vehicle; blue) or ligand stimulation (yellow) conditions. Upper P values are derived from mixed ANCOVA F-test and lower P values reflect pairwise t-test comparisons vs. control group within the linear mixed effects model

negative correlation loop at S6 (pS235/pS236)-IκBα in BD and ASC (**1**), uncoupling of Akt and A/I receptor clusters at PKA RIIβ (pS114) in BD (**2**), the absence of multiple Stat3 (pS727) connections in SCZ (**3**) and increased connections to Zap-70 (pY319)/Syk (pY352) (**4**) and PKC-θ (**5**) in ASC. In B cells (Figure S7), these included increased correlation of Stat1 (pY701) with Stat5 (pY694) in BD and MDD (**1**), uncoupling of Akt and A/I receptor clusters at PKA RIIβ (pS114) in SCZ (**2**) and disruption of the connection between ERK1/2 (pT202/pY204) and p120 Catenin (pT310) in BD (**3**). Taken together, these findings suggest that while the cluster structure of the epitopes within the principal component space is broadly preserved across the clinical groups, there are multiple alterations in the activity-dependent correlation of basal and induced cell signaling epitopes in different neuropsychiatric conditions relative to controls and each other.

Discussion

The current classification of neuropsychiatric conditions reflects clinical syndromes with largely unknown etiology [61, 62]. In this work, we apply high-content functional screening of primary PBMCs from neuropsychiatric patients and typical controls to functionally interrogate the underlying cell signaling structure of different diseases across the neuropsychiatric spectrum. This has a number of implications with respect to interpreting previous molecular profiling analyses and the provision of relevant cellular models for novel drug discovery.

Analysis of individual patient readouts revealed several features in terms of the relative overlap in cell signaling profiles of different neuropsychiatric conditions. First, clustering of individual patient readouts across clinically associated nodes (Fig. 1a) displayed a spectral arrangement (Fig. 1b) of primary peak densities ranging from MDD, through BD and SCZ, to ASC. The overlap of the cell signaling alterations in the different conditions, represented by the proximity of their respective peaks, is largely consistent with the genetic overlap suggested by genome-wide SNP-based genetic correlation studies [9, 10]. This includes a high degree of overlap between SCZ and BD and between BD and MDD, followed by moderate overlap between SCZ and MDD, and SCZ and ASC, and little overlap between MDD and ASC, and BD and ASC. Second, SCZ was the only disease to show a biphasic spectral distribution with a prominent secondary peak within the principal peak areas of MDD and BD. Although we found no significant differences in clinical variables between the two SCZ clusters, this is concurrent with previous studies suggesting heterogeneity in the clinical characteristics of SCZ [9] and the existence of subgroups of patients with distinct molecular pathophysiology [63, 64]. Third, the shallow peak of MDD and wide distribution of MDD patients across the spectrum is consistent with previous reports of increased variation in the molecular etiology of MDD relative to other neuropsychiatric conditions [10]. Finally, although the spectral analysis is useful to determine the relative overlap between the cell signaling profiles of different neuropsychiatric conditions, it enforces a sequential arrangement of the conditions. The linear discriminant analysis (Fig. 1c) further contextualizes this arrangement as a dimensional extension of typical controls.

The present results confirm, but also extend, existing hypotheses of cell signaling alterations in neuropsychiatric conditions. The observed reduction in basal levels of total Akt1 protein in B cells in SCZ (Fig. 2b) is consistent with previous reports in B lymphoblastoid cell lines and post-mortem brain frontal cortex samples from SCZ patients, relative to controls [65], and reports of sensory-motor gating deficits, reminiscent of perceptual alterations in SCZ, in

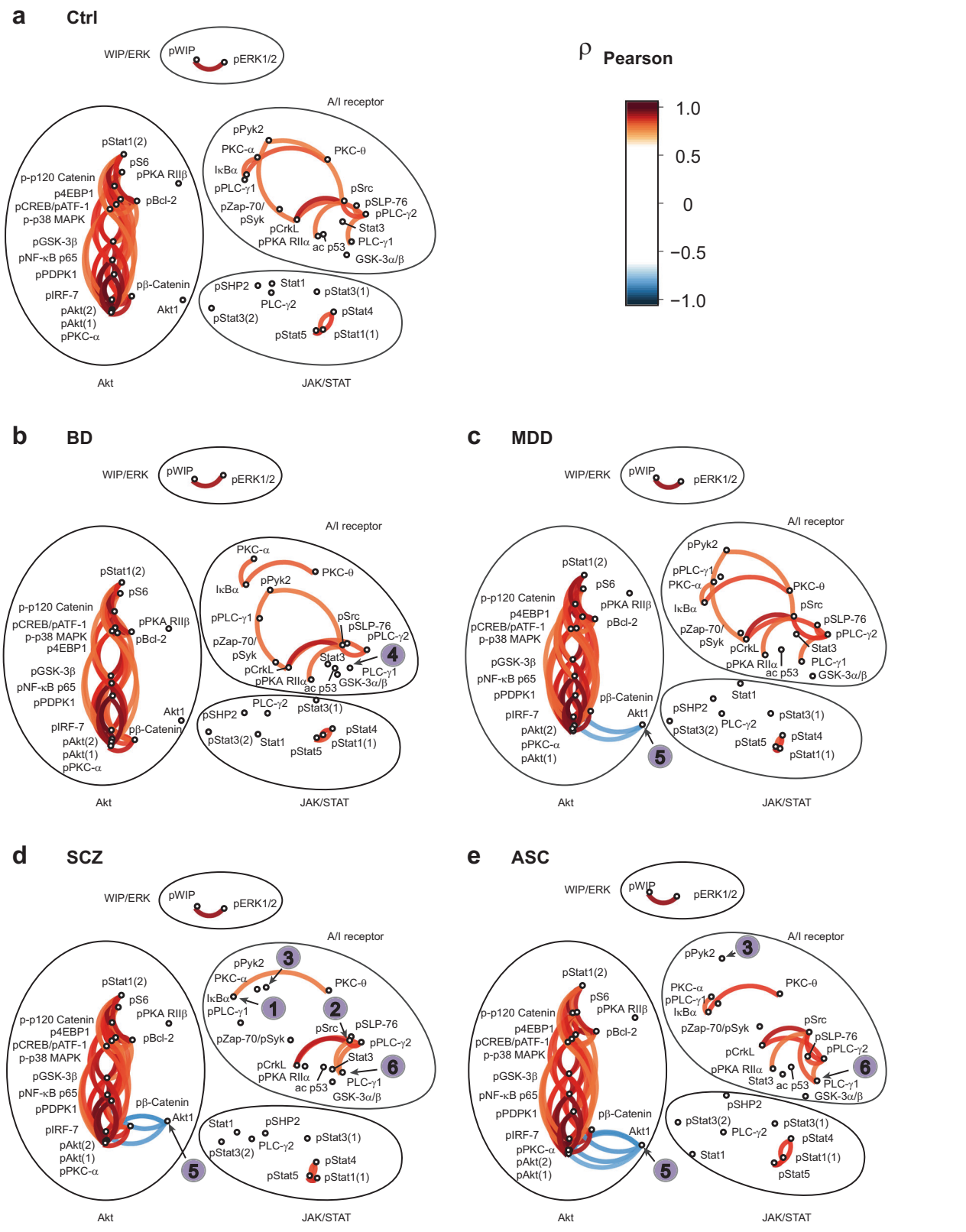

Akt1$^{-/-}$ mice [66]. Furthermore, the present results suggest that Akt1 is functionally dysregulated in SCZ. This is evident from the attenuated response of Akt1 to calyculin A (Fig. 2b) and the increased number of negative correlations between Akt1 and adjacent proteins in the network analysis (Fig. 3). Previous analyses of phospho-specific cell

◀ **Fig. 3** Altered functional correlation structure of cell signaling networks in neuropsychiatric conditions. Cell signaling epitope responses in $CD4^+$ T cells were correlated using data from all ligands and individual donors in each clinical group including (**a**) typical controls (Ctrl; $n = 100$), **b** bipolar disorder (BD; $n = 25$), **c** major depressive disorder (MDD; $n = 25$), **d** schizophrenia (SCZ; $n = 25$), and **e** autism spectrum condition (ASC; $n = 25$). Positive or negative correlations are represented as red or blue connections between epitopes respectively. Legend shows the strength of correlations expressed as Person correlation coefficient, ρ. Only correlations which exceed the Pearson's ρ threshold (≤ -0.8 or ≥ 0.8) are shown. Epitopes are mapped onto broad signaling pathway clusters, annotated with common functionality (Akt, JAK/STAT, antigen/integrin (A/I) receptor, and WIP/ERK), in principal component space. Putative network disconnections present in one or more diseases are labeled as follows: IκBα–PKC-α (**1**), Src (pY418)–PKA RIIα (pS99) (**2**), CrkL (pY207)–Pyk2 (pY402)–Src (pY418) (**3**), and PLC-γ1–PLC-γ2 (**4**). Increased putative network connections include Akt1 with adjacent epitopes (**5**) and Src (pY418)–PLC-γ1 (**6**). Phosphorylation sites for each protein are abbreviated to 'p' for representation and listed in Table S2. Proteins with two phosphorylation sites are abbreviated: pAkt(1), Akt (pT308); pAkt(2), Akt (pS473); pStat1(1), Stat1 (pY701); pStat1(2), Stat1 (pS727); pStat3(1), Stat3 (pY705); pStat3 (2), Stat3 (pS727)

signaling responses suggest that decreases in total protein detection following widespread pathway activation are potentially indicative of negative feedback regulation [25]. Taken together, these findings suggest that previous observations of decreased Akt1 in SCZ are not solely the result of decreased protein expression but are also potentially influenced by an increased negative feedback regulation of the protein in the context of wider signaling network activation. Interestingly, this feature was also shared by ASC and to a lesser extent MDD in the network analysis, suggesting convergent disease mechanisms at the functional level. In contrast, dysregulation of Akt in BD was observed in terms of increased changes in phosphorylation at the Akt activation site pT308 (Fig. 2b) but not in terms of changes in total protein levels or network dysregulation. This is consistent with recent data suggesting that Akt (pT308) is one of the mechanistic targets of the mood stabilizer lithium used to treat BD [67]. Thus, while the present results confirm previous reports of Akt pathway alterations as a common feature of different neuropsychiatric conditions, they suggest that the nature of the alterations, in terms of epitope specificity and regulatory relationships within the cell signaling network, is very different. The results also reveal the importance of using high-content analysis to simultaneously relate changes in total protein levels with those of key phospho-activation sites, a feature recently suggested to be crucial in defining the mechanistic implications of drug response in iPSC-derived neurons of neuropsychiatric patients [68].

In addition to characterizing cell signaling pathways already implicated as primary mediators of neuropsychiatric pathogenesis and drug efficacy, the present results also revealed novel cell signaling targets, S6 (pS235/pS236), NF-κB p65 (pS529), and Stat3 (pS727) (Fig. 2c and Table S6), which were more significantly associated to neuropsychiatric disease. Nodes displaying alterations in NF-κB p65 (pS529) and Stat3 (pS727) activity were shared almost exclusively between SCZ and MDD ($P = 1.8*10^{-5}$, Fisher's exact test probability that overlap occurs by chance). This raises the possibility that NF-κB p65 (pS529) and Stat3 (pS727) might represent a shared substrate for negative symptomatology present in both SCZ and MDD. The identified alterations in NF-κB p65 signaling in PBMCs are consistent with previously reported changes in NF-κB expression in post-mortem brain samples of patients with SCZ [69–71] and MDD [72] and with reports that polymorphisms in the *NFKB1* gene are risk factors for treatment-refractory SCZ [73] and suicide [74]. Concurrently, microglial cell-specific $Stat3^{-/-}$ knockout mice have been reported to show alterations in depressive-like behavior in animal models of major depression [75]. NF-κB and Stat3 are also primary mediators of pro-inflammatory cytokine signaling (e.g., IL-1β, TNF-α, and IL-6) associated with negative symptomatology in both SCZ [63, 76] and MDD [77, 78]. It is possible that these cell signaling alterations in PBMCs in SCZ and MDD are either the result of chronic stimulation with elevated circulating pro-inflammatory cytokines [15, 77] or represent intrinsic cellular phenotypes which are the cause of increased pro-inflammatory cytokine transcription.

The biological implications of these nodes in neuropsychiatric diseases may also extend beyond their involvement in pro-inflammatory pathways. Stat3 has also been shown to regulate the activity-dependent expression and function of key GPCRs and neurotransmitter transporters (e.g., 5HT-2A, β-adreno, GABA, mAch, NMDA, and AMPA receptors [79–82] and the serotonin transporter [83]) in neuronal cells and mediate processes which are reportedly altered neuropsychiatric pathogenesis in the brain (e.g., synaptic plasticity [79], neurogenesis, astrogliogenesis, axonal remodeling [81, 82] and microglial activation [84]). Conversely, NF-κB is reported to mediate the effects of hypothalamic–pituitary–adrenal (HPA) axis dysregulation on stress-induced anhedonia and impaired neurogenesis [85, 86], in addition to regulating the balance between neuroprotective and pro-apoptotic mechanisms in the CNS via NLRP1/NLRP3 inflammasome regulation [87, 88]. Interestingly, modulators of Stat3 (e.g., minocycline, withaferin A, and curcumin) [89–91] and NF-κB (e.g., celecoxib and aspirin) [92, 93] function are currently in clinical trials or have shown efficacy as adjunctive therapies for treating subtypes of neuropsychiatric symptoms, including treatment-resistant negative symptoms in SCZ. This suggests that, in addition to their mechanistic relevance within the CNS, they may also constitute feasible novel drug targets.

The altered phosphorylation responses at S6 (pS235/pS236) in PBMCs are consistent with previous reports of alterations in direct upstream kinases (p70 S6 kinase and p90 S6 kinase) in human post-mortem brain samples of neuropsychiatric patients [94, 95] and behavioral effects in animal models [96–101] of neuropsychiatric diseases. Downstream of mechanistic target of rapamycin complex 1 (mTORC1), the S6 protein represents a key mediator of neuronal activity-dependent synaptic protein synthesis which is implicated in altered synaptic long-term potentiation and long-term depression in different neuropsychiatric disorders [96, 102, 103]. S6 is also involved in modifying adult hippocampal neurogenesis following interactions between GABAergic signaling and neuropsychiatric risk genes in mice [103]. Importantly, the activity of S6 and upstream kinases has been shown to mediate the efficacy of antipsychotic, antidepressant and mood stabilizing drugs [104–106] including several with novel mechanisms of actions [106–110].

Interestingly, the clinically associated cell signaling responses at S6 (pS235/pS236) segregated across different conditions in terms of the respective cell subtypes and ligands involved. Alterations in T-cell subsets ($CD4^+$ and $CD4^-$) using calyculin A and PMA/ionomycin were shared between SCZ and BD, while alterations in B cells using BCR/CD40L and thapsigargin were unique to MDD (Table S6). This raises the possibility that the aberrant responses at S6 (pS235/pS236) in T cells represent a common feature of psychotic conditions while those present in B cells are unique to unipolar depression. The fact that the same epitope is abnormally regulated in different diseases in a mutually exclusive manner, dependent on the cell subtype and stimulant used, suggests that the epitope itself is not the sole pathological determinant. Instead, it likely represents a surrogate endpoint for the integration of abnormal responses across the signaling network. This is supported by the fact that the epitopes which showed the greatest number of clinical associations (S6 (pS235/pS236), NF-κB p65 (pS529) and Stat3 (pS727)) are all distal effectors of their respective canonical signaling pathways (PI3K/mTOR and MAPK/ERK pathways for S6 (pS235/pS236), IL-1 receptor/Toll-like receptor pathway for NF-κB p65 (pS529) and JAK/STAT pathway for Stat3 (pS727)). Concurrently, due to their pleiotropic nature [91, 111, 112], alterations in the activation state of these cell signaling proteins have the potential to affect the transcription and translation of multiple gene products beyond the epitopes measured.

The network correlation analysis across all ligands highlighted further dysregulated epitopes and disease similarities which were not identified by the analysis of individual node responses, such as reduced activity correlations between CrkL (pY207), Pyk2 (pY402), and Src (pY418) in $CD4^+$ T cells in SCZ and ASC (Fig. 3). This suggests that the integration of multiple functional perturbations as changes in network correlation structure can reveal higher order interactions which are not observable through the analysis of individual nodes and reflect a range of potentially pathological signaling states. Interestingly, six out of eight epitopes which showed altered connectivity in $CD4^+$ T cells in SCZ (CrkL (pY207), Pyk2 (pY402), Src (pY418), PKA RIIα (pS99), Akt1, and PLC-γ1; Fig. 3) have previously been associated with response to in vivo clinical antipsychotic therapy [25]. This suggests that the exploration of signaling network correlations ex vivo could provide a novel strategy to identify drug targets with potential in vivo efficacy. Furthermore, by contrasting the distribution of epitopes in functional clusters with changes in individual epitope correlations it is possible to prioritize the putative drug targets in terms of their potential effects on network connectivity.

The present results add to the existing evidence of specific signaling dysregulations in lymphocytes in neuropsychiatric conditions in several ways. First, while previous studies have suggested abnormal expression of cell signaling proteins in resting state PBMCs [65], the present results suggest that basal alterations only account for a minority (20%) of the total cell signaling alterations revealed with the additional use of functional stimulation (Table S6). Furthermore, for nodes which display basal alterations (e.g., basal Akt1 in B cells in SCZ), functional stimulation can be used to accentuate the significance of clinical associations (e.g., calyculin A-Akt1 in B cells in SCZ). Second, previous work has suggested that immune dysregulation in neuropsychiatric conditions involves the composite dysfunction of entire subpopulations of cells [113] or entire pathways within cells [31], in part due to the focus on generic endpoints or single proteins as surrogate markers for whole pathway activation. The fact that the total number of active ligand responses and their fold change distributions were similar between different diseases in each cell subtype (Figure S5 and Table S5) and the number of clinically associated active nodes ($n = 20$) represented a minority (3.4%) of the total active nodes ($n = 581$), suggests that global functionality per cell subtype is largely similar across the clinical groups. This is further supported, at the level of signaling network analysis, by similar cluster composition and functional correlations between the majority of epitopes across clinical groups (Fig. 3 and Figures S6 and S7). Instead, most disease-associated alterations in cell signaling appeared as specific ligand–epitope–cell subtype combinations or changes in individual network connections. These nodes likely represent specific stress points which escape the regulatory control of a wider, more tightly regulated, network and as such represent the most physiologically relevant drug

targets. Moreover, the results allow the prioritization of PBMC subtypes which reflect the most relevant models for future disease investigations. In this respect, it was notable that the majority of clinically associated cell signaling nodes were identified in B cells relative to $CD4^+$ or $CD4^-$ T cells. This is consistent with the enrichment of disease-associated SNPs in B cell subtype-specific promoters in GWAS analyses of selected neuropsychiatric disorders [11].

Finally, the ultimate utility of the identified peripheral cell signaling abnormalities as drug targets will depend on whether they are involved in causal CNS disease mechanisms. Parallel protein changes in patient post-mortem brain studies, behavioral abnormalities in animal knockout/knockin studies and involvement in the mechanisms of clinical drug efficacy, described for several of the identified cell signaling abnormalities, suggest that they may represent plausible surrogate targets with parallel CNS manifestations. Alternatively, the identified cell signaling abnormalities may represent direct targets for treating immunological dysfunctions which can in turn ameliorate brain pathology through peripheral-CNS crosstalk [27, 78]. This is supported by the efficacy of adjunctive immunomodulatory therapies in subgroups of neuropsychiatric patients [114, 115]. In either case, the likelihood that a subset, but not all, of blood-based alterations may influence the CNS and that this may vary across sub-clusters of patients [63], necessitates further investigations to prioritize the identified peripheral cell signaling abnormalities in terms of their potential as novel drug targets. Conversely, candidate compounds will need to be carefully evaluated to ensure that drug interactions outside of the target tissue type do not provoke overt toxicity at the clinical level [116].

While this work aims to provide a proof of principle application for high-content single cell screening in primary patient PBMCs across different neuropsychiatric conditions, several limitations must be taken into account with relevance to future work. First, diagnostic uncertainty and disease heterogeneity between related neuropsychiatric conditions [7, 61, 62] are persistent limitations in the current diagnostic framework. Thus, while study groups were defined, in the absence of alternatives, using clinical assessment of DSM-IV-TR criteria [5], this classification system may potentially be improved by successive incorporation of biological markers (such as those proposed here) which better reflect disease etiology. Second, although the results were controlled for patient medication status as far as possible, the MDD and BD groups consisted primarily of treated patients, limiting interpretation of the results from these groups to putative trait markers of the disease. Third, the depicted network connections (Fig. 3, Figures S6 and S7) represent correlated epitope activity. Further experiments would be required to infer a causative link or direct biochemical binding between the epitopes. Finally, the samples sizes used ($n = 25$ per disease) reflect difficulties in obtaining viable primary PBMCs from strictly defined and well-matched neuropsychiatric patient populations. Future investigations of the identified cell signaling abnormalities would benefit from the inclusion of larger patient cohorts.

In conclusion, the present results allow the definition of convergent abnormal cell signaling phenotypes ("functional cellular endophenotypes") in ex vivo PBMCs from patients with different neuropsychiatric diagnoses. These functional endophenotypes have several potential implications for understanding the molecular etiology of neuropsychiatric diseases and defining novel therapeutic targets. First, they provide a heuristic means to summarize complex genetic risk as tractable and accessible live cell disease models. These models can be applied to novel drug screening [25] and further investigations of disease mechanisms, using complementary molecular profiling techniques and response-based cell sorting. Second, they provide a means for functionally testing clinical drugs against disease-related cellular phenotypes in live patient samples ex vivo for the purposes of treatment response prediction and personalized medicine [25]. Third, as the molecular heterogeneity of neuropsychiatric diseases becomes increasingly apparent [61], they offer novel strategies for defining subgroups of patients with potentially distinct molecular etiology and pharmacological response profiles. Finally, they provide a means for discerning functional responses which are unique to specific conditions (e.g., thapsigargin-S6 (pS235/pS236) in B cells in MDD) or alternatively shared between conditions (e.g., calyculin A-S6 (pS235/pS236) in $CD4^-$ T cells in SCZ and BD) with subsets of closely related symptoms (e.g., psychosis and mania respectively). At a time when the diagnostic framework of neuropsychiatric conditions is constantly evolving [2], these functional endophenotypes may serve to facilitate both the redefinition of diagnostic categories and the elucidation of drug targets and treatment response predictors which transcend diagnostic boundaries.

Acknowledgements We would like to thank clinicians and support staff at the affiliated institutions for patient recruitment and sample collection, including Liliana Ruta and Stephanie Mok for the ASC cohort; Eva Brombacher for sample preparation; collaborators Joshua A. Bishop, Tracey Petryshen, and Steven J. Haggarty from Harvard Medical School (Boston, MA, USA) for contribution of the JB1121 compound; and PBMC donors for provision of biological samples.

Funding This work was supported by grants to S.B. from the Stanley Medical Research Institute (SMRI) and the Engineering and Physical Sciences Research Council UK (EPSRC CASE studentship and Impact Acceleration Award). S.G.L. was supported an by EPSRC CASE studentship and Psynova Neurotech Ltd. J.T. was supported through grants awarded t`o Psynova Neurotech Ltd. by the European Union FP7 funding scheme: Marie Curie Actions Industry-Academia Partnerships and Pathways (ref. 286334, PSYCH-AID project); by the Virgo consortium, funded by the Dutch Government (ref. FES0908); by the Netherlands Genomics Initiative (ref. 050-060); and by the

Dutch Fund for Economic Structure Reinforcement, the NeuroBasic PharmaPhenomics project (ref. 0908). S.B.-C. and B.A. were supported by the Autism Research Trust.

Compliance with ethical standards

Conflict of interest J.T. was a consultant for Psynova Neurotech Ltd. until April 2016. S.G.L. was part funded by Psynova Neurotech Ltd. until October 2015. S.B is a director of Psynova Neurotech Ltd. and Psyomics Ltd. The remaining authors declare that they have no conflict of interest.

References

1. Benes FM. Searching for unique endophenotypes for schizophrenia and bipolar disorder within neural circuits and their molecular regulatory mechanisms. Schizophr Bull. 2007;33:932–6.
2. Adam D. On the spectrum. Nature. 2013;496:6–8.
3. Falkai P, Rossner MJ, Schulze TG, Hasan A, Brzózka MM, Malchow B, et al. Kraepelin revisited: schizophrenia from degeneration to failed regeneration. Mol Psychiatry. 2015;20:671–6.
4. Meyer U, Feldon J, Dammann O. Schizophrenia and autism: both shared and disorder-specific pathogenesis via perinatal inflammation? Pediatr Res. 2011;69:26R–33R.
5. American Psychiatric Association [APA]. The diagnostic and statistical manual of mental disorders. 4th ed., text revision (DSM-IV-TR). Author: Washington, DC, 2000.
6. Schwarz E, Bahn S, The utility of biomarker discovery approaches for the detection of disease mechanisms in psychiatric disorders. Br J Pharmacol. 2008;153:S133–6.
7. Bromet EJ, Kotov R, Fochtmann LJ, Carlson Ga, Tanenberg-Karant M, Ruggero C, et al. Diagnostic shifts during the decade following first admission for psychosis. Am J Psychiatry. 2011;168:1186–94.
8. Lally J, MacCabe JH. Antipsychotic medication in schizophrenia: a review. Br Med Bull. 2015;114:169–79.
9. Kahn RS, Sommer IE, Murray RM, Meyer-Lindenberg A, Weinberger DR, Cannon TD, et al. Schizophrenia. Nat Rev Dis Prim. 2015;1:15067.
10. Lee SH, Ripke S, Neale BM, Faraone SV, Purcell SM, Perlis RH, et al. Genetic relationship between five psychiatric disorders estimated from genome-wide SNPs. Nat Genet. 2013;45:984–94.
11. Ripke S, Neale BM, Corvin A, Walters JTR, Farh K-H, Holmans PA, et al. Biological insights from 108 schizophrenia-associated genetic loci. Nature. 2014;511:421–7.
12. Purcell SM, Moran JL, Fromer M, Ruderfer D, Solovieff N, Roussos P, et al. A polygenic burden of rare disruptive mutations in schizophrenia. Nature. 2014;506:185–90.
13. Rees E, Walters JTR, Georgieva L, Isles AR, Chambert KD, Richards AL, et al. Analysis of copy number variations at 15 schizophrenia-associated loci. Br J Psychiatry. 2014;204:108–14.
14. Cross-Disorder Group of the Psychiatric Genomics Consortium. Identification of risk loci with shared effects on five major psychiatric disorders: a genome-wide analysis. Lancet. 2013;381:1371–9.
15. Miller BJ, Buckley P, Seabolt W, Mellor A, Kirkpatrick B. Meta-analysis of cytokine alterations in schizophrenia: clinical status and antipsychotic effects. Biol Psychiatry. 2011;70:663–71.
16. Herberth M, Koethe D, Cheng TMK, Krzyszton ND, Schoeffmann S, Guest PC, et al. Impaired glycolytic response in peripheral blood mononuclear cells of first-onset antipsychotic-naive schizophrenia patients. Mol Psychiatry. 2011;16:848–59.
17. van Beveren NJM, Buitendijk GHS, Swagemakers S, Krab LC, Röder C, de Haan L et al. Marked reduction of AKT1 expression and deregulation of AKT1-associated pathways in peripheral blood mononuclear cells of schizophrenia patients. PLoS ONE. 2012;7:e32618.
18. Brennand KJ, Simone A, Jou J, Gelboin-Burkhart C, Tran N, Sangar S, et al. Modelling schizophrenia using human induced pluripotent stem cells. Nature. 2011;473:221–5.
19. Mertens J, Wang Q-W, Kim Y, Yu DX, Pham S, Yang B, et al. Differential responses to lithium in hyperexcitable neurons from patients with bipolar disorder. Nature. 2015;527:95–9.
20. Sellgren CM, Sheridan SD, Gracias J, Xuan D, Fu T, Perlis RH. Patient-specific models of microglia-mediated engulfment of synapses and neural progenitors. Mol Psychiatry. 2017;22:170–7.
21. Martins-Taylor K, Xu R-H. Concise review: genomic stability of human induced pluripotent stem cells. Stem Cells. 2012;30:22–7.
22. Cundiff PE, Anderson SA. Impact of induced pluripotent stem cells on the study of central nervous system disease. Curr Opin Genet Dev. 2011;21:354–61.
23. Falk A, Heine VM, Harwood AJ, Sullivan PF, Peitz M, Brüstle O et al. Modeling psychiatric disorders: from genomic findings to cellular phenotypes. Mol Psychiatry. 2016;21:1167–79.
24. Gladkevich A, Kauffman HF, Korf J. Lymphocytes as a neural probe: potential for studying psychiatric disorders. Prog Neuropsychopharmacol Biol Psychiatry. 2004;28:559–76.
25. Lago SG, Tomasik J, van Rees GF, Steeb H, Cox DA, Rustogi N et al. Drug discovery in neuropsychiatric disorders using high-content single-cell screening of signaling network responses ex vivo. Submitted. 2018.
26. Rogers GB, Keating DJ, Young RL, Wong ML, Licinio J, Wesselingh S. From gut dysbiosis to altered brain function and mental illness: mechanisms and pathways. Mol Psychiatry. 2016;21:738–48.
27. Dantzer R, O'Connor JC, Freund GG, Johnson RW, Kelley KW. From inflammation to sickness and depression: when the immune system subjugates the brain. Nat Rev Neurosci. 2008;9:46–56.
28. Dunn AJ, Swiergiel AH, De Beaurepaire R. Cytokines as mediators of depression: what can we learn from animal studies? Neurosci Biobehav Rev. 2005;29:891–909.
29. Irish JM, Hovland R, Krutzik PO, Perez OD, Bruserud Ø, Gjertsen BT, et al. Single cell profiling of potentiated phospho-protein networks in cancer cells. Cell. 2004;118:217–28.
30. O'Gorman WE, Hsieh EWY, Savig ES, Gherardini PF, Hernandez JD, Hansmann L, et al. Single-cell systems-level analysis of human Toll-like receptor activation defines a chemokine signature in patients with systemic lupus erythematosus. J Allergy Clin Immunol. 2015;136:1326–36.

31. Sullivan PF. Puzzling over schizophrenia: schizophrenia as a pathway disease. Nat Med. 2012;18:210–1.
32. Hopkins AL, Groom CR. The druggable genome. Nat Rev Drug Discov. 2002;1:727–30.
33. Zheng W, Thorne N, McKew JC. Phenotypic screens as a renewed approach for drug discovery. Drug Discov Today. 2013;18:1067–73.
34. Krutzik PO, Nolan GP Fluorescent cell barcoding in flow cytometry allows high-throughput drug screening and signaling profiling. Nat Methods. 2006;3:361–8.
35. Krutzik PO, Crane JM, Clutter MR, Nolan GP. High-content single-cell drug screening with phosphospecific flow cytometry. Nat Chem Biol. 2008;4:132–42.
36. World Medical Association. World Medical Association Declaration of Helsinki: ethical principles for medical research involving human subjects. JAMA. 2013;310:2191–4.
37. Bossuyt PM, Reitsma JB, Bruns DE, Gatsonis CA, Glasziou PP, Irwig LM, et al. Towards complete and accurate reporting of studies of diagnostic accuracy: the STARD initiative. Radiology. 2003;226:24–8.
38. Wagner FF, Bishop JA, Gale JP, Shi X, Walk M, Ketterman J, et al. Inhibitors of glycogen synthase kinase 3 with exquisite kinome-wide selectivity and their functional effects. ACS Chem Biol. 2016;11:1952–63.
39. R Core Team. R: a language and environment for statistical computing. R Foundation for Statistical Computing: Vienna, Austria, 2017.
40. Leek JT, Johnson WE, Parker HS, Jaffe AE, Storey JD. The sva package for removing batch effects and other unwanted variation in high-throughput experiments. Bioinformatics. 2012;28:882–3.
41. Johnson WE, Li C, Rabinovic A. Adjusting batch effects in microarray expression data using empirical Bayes methods. Biostatistics. 2007;8:118–27.
42. Björklund ÅK, Forkel M, Picelli S, Konya V, Theorell J, Friberg D, et al. The heterogeneity of human CD127+ innate lymphoid cells revealed by single-cell RNA sequencing. Nat Immunol. 2016;17:451–60.
43. Yanez LZ, Han J, Behr BB, Reijo Pera RA, Camarillo DB. Human oocyte developmental potential is predicted by mechanical properties within hours after fertilization. Nat Commun. 2016;7:10809.
44. Van Keymeulen A, Lee MY, Ousset M, Brohée S, Rorive S, Giraddi RR, et al. Reactivation of multipotency by oncogenic PIK3CA induces breast tumour heterogeneity. Nature. 2015;525:119–23.
45. Li S, Łabaj PP, Zumbo P, Sykacek P, Shi W, Shi L, et al. Detecting and correcting systematic variation in large-scale RNA sequencing data. Nat Biotechnol. 2014;32:888–95.
46. Bailey P, Chang DK, Nones K, Johns AL, Patch AM, Gingras MC, et al. Genomic analyses identify molecular subtypes of pancreatic cancer. Nature. 2016;531:47–52.
47. Tamplin OJ, Durand EM, Carr LA, Childs SJ, Hagedorn EJ, Li P, et al. Hematopoietic stem cell arrival triggers dynamic remodeling of the perivascular niche. Cell. 2015;160:241–52.
48. Sweeney TE, Shidham A, Wong HR, Khatri P. A comprehensive time-course-based multicohort analysis of sepsis and sterile inflammation reveals a robust diagnostic gene set. Sci Transl Med. 2015;7:287ra71.
49. Bai H, Harmancı AS, Erson-Omay EZ, Li J, Coşkun S, Simon M, et al. Integrated genomic characterization of IDH1-mutant glioma malignant progression. Nat Genet. 2016;48:59–66.
50. Benjamini Y, Hochberg Y. Controlling the false discovery rate: a practical and powerful approach to multiple testing. J R Stat Soc B. 1995;57:289–300.
51. Bendall SC, Simonds EF, Qiu P, Amir ED, Krutzik PO, Finck R, et al. Single-cell mass cytometry of differential immune and drug responses across a human hematopoietic continuum. Science. 2011;332:687–96.
52. Bodenmiller B, Zunder ER, Finck R, Chen TJ, Savig ES, Bruggner RV, et al. Multiplexed mass cytometry profiling of cellular states perturbed by small-molecule regulators. Nat Biotechnol. 2012;30:858–67.
53. Maiese K, Chong ZZ, Shang YC, Wang S. MTOR: on target for novel therapeutic strategies in the nervous system. Trends Mol Med. 2013;19:51–60.
54. Delghandi MP, Johannessen M, Moens U. The cAMP signalling pathway activates CREB through PKA, p38 and MSK1 in NIH 3T3 cells. Cell Signal. 2005;17:1343–51.
55. Chen J-F, Eltzschig HK, Fredholm BB. Adenosine receptors as drug targets — what are the challenges? Nat Rev Drug Discov. 2013;12:265–86.
56. Brownlie RJ, Zamoyska R. T cell receptor signalling networks: branched, diversified and bounded. Nat Rev Immunol. 2013;13:257–69.
57. Kalland ME, Oberprieler NG, Vang T, Taskén K, Torgersen KM. T cell-signaling network analysis reveals distinct differences between CD28 and CD2 costimulation responses in various subsets and in the MAPK pathway between resting and activated regulatory T cells. J Immunol. 2011;187:5233–45.
58. Niiro H, Clark EA. Regulation of B-cell fate by antigen-receptor signals. Nat Rev Immunol. 2002;2:945-56.
59. Young RM, Staudt LM. Targeting pathological B cell receptor signalling in lymphoid malignancies. Nat Rev Drug Discov. 2013;12:229–43.
60. Davies R, Vogelsang P, Jonsson R, Appel S. An optimized multiplex flow cytometry protocol for the analysis of intracellular signaling in peripheral blood mononuclear cells. J Immunol Methods. 2016;436:58-63.
61. Agid Y, Buzsáki G, Diamond DM, Frackowiak R, Giedd J, Girault J-A, et al. How can drug discovery for psychiatric disorders be improved? Nat Rev Drug Discov. 2007;6:189–201.
62. Hyman SE. A glimmer of light for neuropsychiatric disorders. Nature. 2008;455:890–3.
63. Fillman SG, Weickert TW, Lenroot RK, Catts SV, Bruggemann JM, Catts VS et al. Elevated peripheral cytokines characterize a subgroup of people with schizophrenia displaying poor verbal fluency and reduced Broca's area volume. Mol Psychiatry. 2016;21:1090-8.
64. Edwards AC, Bigdeli TB, Docherty AR, Bacanu S, Lee D, de Candia TR, et al. Meta-analysis of positive and negative symptoms reveals schizophrenia modifier genes. Schizophr Bull. 2016;42:279–87.
65. Emamian ES, Hall D, Birnbaum MJ, Karayiorgou M, Gogos JA. Convergent evidence for impaired AKT1-GSK3beta signaling in schizophrenia. Nat Genet. 2004;36:131–7.
66. Beaulieu J-M. A role for Akt and glycogen synthase kinase-3 as integrators of dopamine and serotonin neurotransmission in mental health. J Psychiatry Neurosci. 2012;37:7–16.
67. Pan JQ, Lewis MC, Ketterman JK, Clore EL, Riley M, Richards KR, et al. AKT kinase activity is required for lithium to modulate mood-related behaviors in mice. Neuropsychopharmacology. 2011;36:1397–411.
68. Tobe BTD, Crain AM, Winquist AM, Calabrese B, Makihara H, Zhao WN, et al. Probing the lithium-response pathway in hiPSCs implicates the phosphoregulatory set-point for a cytoskeletal modulator in bipolar pathogenesis. Proc Natl Acad Sci USA. 2017;114:E4462-E4471.
69. Volk DW, Chitrapu A, Edelson JR, Roman KM, Moroco AE, Lewis DA. Molecular mechanisms and timing of cortical immune activation in schizophrenia. Am J Psychiatry. 2015;172:1112–21.

70. García-Bueno B, Gassó P, MacDowell KS, Callado LF, Mas S, Bernardo M, et al. Evidence of activation of the Toll-like receptor-4 proinflammatory pathway in patients with schizophrenia. J Psychiatry Neurosci. 2016;41:E46–55.
71. Roussos P, Katsel P, Davis KL, Giakoumaki SG, Lencz T, Malhotra AK, et al. Convergent findings for abnormalities of the NF-κB signaling pathway in schizophrenia. Neuropsychopharmacology. 2013;38:533–9.
72. Malki K, Pain O, Tosto MG, Du Rietz E, Carboni L, Schalkwyk LC. Identification of genes and gene pathways associated with major depressive disorder by integrative brain analysis of rat and human prefrontal cortex transcriptomes. Transl Psychiatry. 2015;5:e519.
73. Liou Y-J, Wang H-H, Lee M-TM, Wang S-C, Chiang H-L, Chen C-C, et al. Genome-wide association study of treatment refractory schizophrenia in Han Chinese. PLoS ONE. 2012;7:e33598.
74. Coon H, Darlington T, Pimentel R, Smith KR, Huff CD, Hu H, et al. Genetic risk factors in two Utah pedigrees at high risk for suicide. Transl Psychiatry. 2013;3:e325.
75. Kwon S-H, Han J-K, Choi M, Kwon Y-J, Kim SJ, Yi EH, et al. Dysfunction of microglial STAT3 alleviates depressive behavior via neuron-microglia interactions. Neuropsychopharmacology. 2017;42:2072-86.
76. Fillman SG, Cloonan N, Catts VS, Miller LC, Wong J, McCrossin T, et al. Increased inflammatory markers identified in the dorsolateral prefrontal cortex of individuals with schizophrenia. Mol Psychiatry. 2013;18:206–14.
77. Felger JC, Lotrich FE. Inflammatory cytokines in depression: neurobiological mechanisms and therapeutic implications. Neuroscience. 2013;246:199–229.
78. Dean B. Understanding the role of inflammatory-related pathways in the pathophysiology and treatment of psychiatric disorders: evidence from human peripheral studies and CNS studies. Int J Neuropsychopharmacol. 2011;14:997–1012.
79. Nicolas CS, Peineau S, Amici M, Csaba Z, Fafouri A, Javalet C, et al. The Jak/STAT pathway is involved in synaptic plasticity. Neuron. 2012;73:374–90.
80. Berridge MJ. Calcium signalling and psychiatric disease: bipolar disorder and schizophrenia. Cell Tissue Res. 2014;357:477–92.
81. Nicolas CS, Amici M, Bortolotto ZA, Doherty A, Csaba Z, Fafouri A, et al. The role of JAK-STAT signaling within the CNS. JAKSTAT. 2013;2:e22925.
82. Murase S, McKay RD. Neuronal activity-dependent STAT3 localization to nucleus is dependent on Tyr-705 and Ser-727 phosphorylation in rat hippocampal neurons. Eur J Neurosci. 2014;39:557–65.
83. Kong E, Sucic S, Monje FJ, Savalli G, Diao W, Khan D, et al. STAT3 controls IL6-dependent regulation of serotonin transporter function and depression-like behavior. Sci Rep. 2015;5:9009.
84. Hu X, Leak RK, Shi Y, Suenaga J, Gao Y, Zheng P, et al. Microglial and macrophage polarization—new prospects for brain repair. Nat Rev Neurol. 2015;11:56–64.
85. Koo JW, Russo SJ, Ferguson D, Nestler EJ, Duman RS. Nuclear factor-B is a critical mediator of stress-impaired neurogenesis and depressive behavior. Proc Natl Acad Sci USA. 2010;107:2669–74.
86. Miller GE, Chen E, Sze J, Marin T, Arevalo JMG, Doll R, et al. A functional genomic fingerprint of chronic stress in humans: blunted glucocorticoid and increased NF-κB signaling. Biol Psychiatry. 2008;64:266–72.
87. Lipton SA. Janus faces of NF-kappa B: neurodestruction versus neuroprotection. Nat Med. 1997;3:20–2.
88. Datta-Mitra A, Kundu-Raychaudhuri S, Mitra A, Raychaudhuri SP. Cross talk between neuroregulatory molecule and monocyte: nerve growth factor activates the inflammasome. PLoS ONE. 2015;10:e0121626.
89. Zhang L, Zhao J. Profile of minocycline and its potential in the treatment of schizophrenia. Neuropsychiatr Dis Treat. 2014;10:1103–11.
90. Oya K, Kishi T, Iwata N. Efficacy and tolerability of minocycline augmentation therapy in schizophrenia: a systematic review and meta-analysis of randomized controlled trials. Hum Psychopharmacol. 2014;29:483–91.
91. Miklossy G, Hilliard TS, Turkson J. Therapeutic modulators of STAT signalling for human diseases. Nat Rev Drug Discov. 2013;12:611–29.
92. Zheng W, Cai DB, Yang XH, Ungvari GS, Ng CH, Müller N, et al. Adjunctive celecoxib for schizophrenia: a meta-analysis of randomized, double-blind, placebo-controlled trials. J Psychiatr Res. 2017;92:139–46.
93. Sommer IE, de Witte L, Begemann M, Kahn RS. Nonsteroidal anti-inflammatory drugs in schizophrenia. J Clin Psychiatry. 2012;73:414–9.
94. Jernigan CS, Goswami DB, Austin MC, Iyo AH, Chandran A, Stockmeier CA, et al. The mTOR signaling pathway in the prefrontal cortex is compromised in major depressive disorder. Prog Neuropsychopharmacol Biol Psychiatry. 2011;35:1774–9.
95. Yuan P, Zhou R, Wang Y, Li X, Li J, Chen G, et al. Altered levels of extracellular signal-regulated kinase signaling proteins in postmortem frontal cortex of individuals with mood disorders and schizophrenia. J Affect Disord. 2010;124:164–9.
96. Dwyer JM, Maldonado-Avilés JG, Lepack AE, DiLeone RJ, Duman RS. Ribosomal protein S6 kinase 1 signaling in prefrontal cortex controls depressive behavior. Proc Natl Acad Sci USA. 2015;112:6188–93.
97. Kim SH, Park HG, Kim HS, Ahn YM, Kim YS. Effects of neonatal MK-801 treatment on p70S6K-S6/eIF4B signal pathways and protein translation in the frontal cortex of the developing rat brain. Int J Neuropsychopharmacol. 2010;13:1233–46.
98. Sawicka K, Pyronneau A, Chao M, Bennett MVL, Zukin RS. Elevated ERK/p90 ribosomal S6 kinase activity underlies audiogenic seizure susceptibility in fragile X mice. Proc Natl Acad Sci USA. 2016;113:E6290–E6297.
99. Bhattacharya A, Mamcarz M, Mullins C, Choudhury A, Boyle RG, Smith DG, et al. Targeting translation control with p70 S6 kinase 1 inhibitors to reverse phenotypes in fragile X syndrome mice. Neuropsychopharmacology. 2016;41:1991-2000.
100. Engel SR, Creson TK, Hao Y, Shen Y, Maeng S, Nekrasova T, et al. The extracellular signal-regulated kinase pathway contributes to the control of behavioral excitement. Mol Psychiatry. 2009;14:448–61.
101. Biever A, Valjent E, Puighermanal E. Ribosomal protein S6 phosphorylation in the nervous system: from regulation to function. Front Mol Neurosci. 2015;8:75.
102. Feliciano DM, Lin TV, Hartman NW, Bartley CM, Kubera C, Hsieh L, et al. A circuitry and biochemical basis for tuberous sclerosis symptoms: from epilepsy to neurocognitive deficits. Int J Dev Neurosci. 2013;31:667–78.
103. Costa-Mattioli M, Monteggia LM. mTOR complexes in neurodevelopmental and neuropsychiatric disorders. Nat Neurosci. 2013;16:1537–43.
104. Einat H, Yuan P, Gould TD, Li J, Du J, Zhang L, et al. The role of the extracellular signal-regulated kinase signaling pathway in mood modulation. J Neurosci. 2003;23:7311–6.
105. Pereira A, Zhang B, Malcolm P, Sundram S. Clozapine regulation of p90RSK and c-Fos signaling via the ErbB1-ERK pathway is distinct from olanzapine and haloperidol in mouse cortex and striatum. Prog Neuropsychopharmacol Biol Psychiatry. 2013;40:353–63.

106. Ignácio ZM, Réus GZ, Arent CO, Abelaira HM, Pitcher MR, Quevedo J. New perspectives on the involvement of mTOR in depression as well as in the action of antidepressant drugs. Br J Clin Pharmacol. 2016;82:1280-1290.
107. Naughton M, Clarke G, O'Leary OF, Cryan JF, Dinan TG. A review of ketamine in affective disorders: current evidence of clinical efficacy, limitations of use and pre-clinical evidence on proposed mechanisms of action. J Affect Disord. 2014;156: 24–35.
108. Caddy C, Giaroli G, White TP, Shergill SS, Tracy DK. Ketamine as the prototype glutamatergic antidepressant: pharmacodynamic actions, and a systematic review and meta-analysis of efficacy. Ther Adv Psychopharmacol. 2014;4:75–99.
109. Dong J, Zhou Q, Wei Z, Yan S, Sun F, Cai X. Protein kinase A mediates scopolamine-induced mTOR activation and an antidepressant response. J Affect Disord. 2018;227:633–42.
110. Koike H, Iijima M, Chaki S. Involvement of the mammalian target of rapamycin signaling in the antidepressant-like effect of group II metabotropic glutamate receptor antagonists. Neuropharmacology. 2011;61:1419–23.
111. Laplante M, Sabatini DM. mTOR signaling at a glance. J Cell Sci. 2009;122:3589–94.
112. Oeckinghaus A, Hayden MS, Ghosh S. Crosstalk in NF-κB signaling pathways. Nat Immunol. 2011;12:695–708.
113. Guo J, Liu C, Wang Y, Feng B, Zhang X. Role of T helper lymphokines in the immune-inflammatory pathophysiology of schizophrenia: Systematic review and meta-analysis. Nord J Psychiatry. 2015;69:364–72.
114. Fond G, Hamdani N, Kapczinski F, Boukouaci W, Drancourt N, Dargel A, et al. Effectiveness and tolerance of anti-inflammatory drugs' add-on therapy in major mental disorders: a systematic qualitative review. Acta Psychiatr Scand. 2014; 129:163–79.
115. Sommer IE, van Westrhenen R, Begemann MJH, de Witte LD, Leucht S, Kahn RS. Efficacy of anti-inflammatory agents to improve symptoms in patients with schizophrenia: an update. Schizophr Bull. 2014;40:181–91.
116. Pereira A, McLaren A, Bell WR, Copolov D, Dean B. Potential clozapine target sites on peripheral hematopoietic cells and stromal cells of the bone marrow. Pharmacogenomics J. 2003;3:227–34.